Exploitation of a Particle Swarm Optimization Algorithm for Designing a Lightweight Parallel Hybrid Electric Vehicle

Publisher copyright

(Article begins on next page)

20 April 2024

Article

Exploitation of a Particle Swarm Optimization Algorithm for Designing a Lightweight Parallel Hybrid Electric Vehicle

Matteo Spano [1,2,*], Pier Giuseppe Anselma [1,2], Daniela Anna Misul [2,3] and Giovanni Belingardi [1,2]

[1] Department of Mechanical and Aerospace Engineering (DIMEAS), Politecnico di Torino, 10125 Torino, Italy; pier.anselma@polito.it (P.G.A.); giovanni.belingardi@polito.it (G.B.)
[2] Center of Automotive Research and Sustainable mobility (CARS), Politecnico di Torino, 10125 Torino, Italy; daniela.misul@polito.it
[3] Department of Energetic (DENERG), Politecnico di Torino, 10125 Torino, Italy
[*] Correspondence: matteo.spano@polito.it

Abstract: The dramatic global climate change has driven governments to drastically tackle pollutant emissions. In the transportation field, one of the technological responses has been powertrain electrification for passengers' cars. Nevertheless, the large amount of possible powertrain designs does not help the development of an exhaustive sizing process. In this research, a multi-objective particle swarm optimization algorithm is proposed to find the optimal layout of a parallel P2 hybrid electric vehicle powertrain with the aim of maximizing fuel economy capability and minimizing production cost. A dynamic programming-based algorithm is used to ensure the optimal vehicle-level energy management. The results show that diverse powertrain layouts may be suggested when different weights are assigned to the sizing targets related to fuel economy and production cost, respectively. Particularly, upsizing the power sources and increasing the number of gears might be advised to enhance HEV fuel economy capability through the efficient exploitation of the internal combustion engine (ICE) operation. On the other hand, reduction of the HEV production cost could be achieved by downsizing the power sources and limiting the number of gears with respect to conventional ICE-powered vehicles thanks to the interaction between ICE and electric motor.

Keywords: hybrid electric vehicle (HEV); design; optimal layout; multi-objective particle swarm optimization (PSO)

1. Introduction

The impellent need to decrease greenhouse gases (GHGs) emissions is driving car manufacturers towards different propulsion systems. In the last decade, the internal combustion engine (ICE) has often been coupled with electrical components in order to reduce its fuel consumption and, consequently, its pollution. In this context, hybrid electric vehicles (HEVs) are being developed by most car manufacturers owing to their interesting trade-off between fuel efficiency, drivability, and CO_2 emissions [1]. Nevertheless, the presence of different power sources along with the additional components for implementing the electric drive do impact the design process of HEVs. To find a globally optimal and universally accepted development method still represents an open question [2].

A lot of research has recently been conducted worldwide to address this problem. Fuel economy (FE) variability (i.e., the variation in fuel economy due to different driving styles, traffic conditions, and so on) has been studied and addressed in [3], hence providing a design method capable of reducing the variability in FE by up to 34% with respect to a standard process. A clutch-less multimode parallel HEV (CMP-HEV) has been firstly introduced in [4] and then its design parameters have been studied in [5], providing interesting FE and acceleration performance analyses. The battery degradation and its effect on fuel economy and total cost of ownership (TCO) have been considered in [6] for the design methodology of a heavy-duty HEV.

Evolutionary algorithms (EAs) have been exploited for sizing HEVs thanks to their capability of thoroughly exploring the design space. As an example, a heavy-duty series HEV is sized using chaos-enhanced accelerated particle swarm optimization (CA PSO) in [7], outperforming the standard PSO and providing an interesting design method. In [8], a light-duty parallel HEV is designed using three different derivative-free optimization algorithms (i.e., divided rectangles, simulated annealing, and genetic algorithm) and a hybrid method, obtaining improvements in fuel consumption when comparing the results with the initial HEV layout.

Nevertheless, to the best of the authors' knowledge, the previous works in the literature have not always completely assessed the light-duty HEV design problem. Indeed, they often focused specifically on achieving high fuel economy without accurately addressing the production costs and/or they did not exhaustively explore the whole design space. Moreover, not many studies take into account a lower number of gears than the standard (i.e., five or six gears for passenger cars).

In a recent study of the authors [9], a comparison of different numbers of gears in a parallel HEV has been brought up, based upon economic considerations taking into account both the lifetime operative cost and transmission cost. The cooperation of the electric machine (EM) with the ICE was demonstrated to be capable of balancing a lower number of gears compared with a conventional vehicle (i.e., propelled by the ICE alone) while assessing the fuel economy.

Starting from the reviewed studies, the objective here is to provide an exhaustive methodology to assess the performances of an HEV by means of various analyses. Evaluation metrics include not only vehicle performance such as acceleration capability and estimated fuel consumption, but also the production cost of chassis, battery, ICE, EM, and transmission, thus addressing the optimal HEV powertrain design problem considering different targets. To this end, a multi-objective PSO algorithm is used at the vehicle design level for efficiently sizing the different components in the HEV powertrain architecture. Then, dynamic programming (DP) is used at the powertrain control level for the optimal choice of driving mode, gear selection, and power split between ICE and EM, retaining both a standard drive cycle and different real-world driving missions. This particular optimization strategy and the interaction between the two HEV powertrain objectives (i.e., component design and powertrain control) can be referred to as bi-nested [10], and in this context, the DP has already been used to reach an optimal solution for different control problems [11,12].

The remainder of this article outlines firstly the methodology for assessing the drivability, the acceleration performance, and the fuel economy. This is followed by an explanation of the implemented PSO workflow and its objectives. Then, the results obtained are shown and discussed. Finally, the conclusions of this study are provided.

2. HEV Modelling and Control

In this section, firstly, the HEV modelling and architecture will be presented with all the main equations used in the study of the vehicle behavior. Then, the DP algorithm used at the control level will be shown.

2.1. HEV Architecture and Model

The HEV architecture chosen for this study is a full HEV parallel P2, having the EM located after the ICE right before the automated manual transmission. The parallel P2 HEV exhibits an interesting trade-off between energy consumption and ease of production owing to a limited difference with respect to a conventional ICE-powered vehicle [13]. This HEV architecture enables three ways of providing torque to the wheels: (1) pure electric mode and (2) pure thermal mode, i.e., when either the EM or the ICE solely deliver the total amount of power requested, respectively; (3) torque split mode, which is when both of the power sources contribute to providing the torque. A particular torque split mode relates to battery charging for which the ICE provides extra power compared with the

value required to overcome the total requirement of the wheels in order to supply charging power to the battery. All the main components of this HEV powertrain architecture are illustrated in Figure 1. A gear ratio between the ICE and the transmission allows increasing the torque delivered by the former. A clutch is embedded that is disengaged when driving in pure electric mode. Moreover, the main data used for virtually simulating a compact size HEV are found in Table 1.
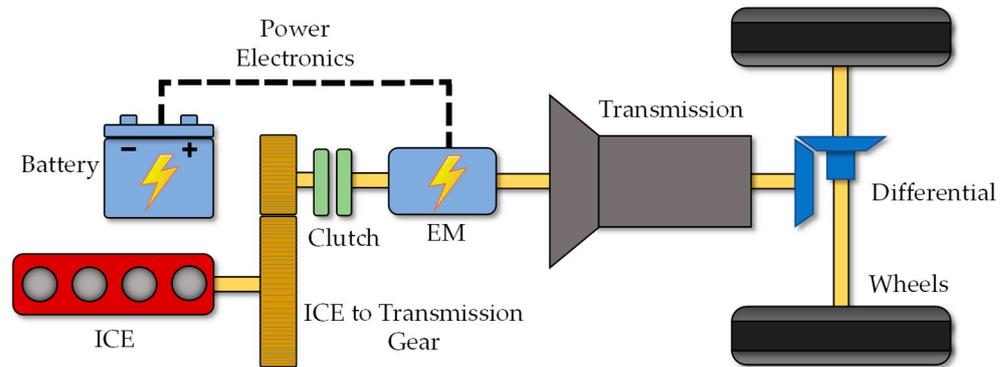

Figure 1. Parallel P2 full hybrid electric vehicle (HEV) architecture.

Table 1. Hybrid electric vehicle (HEV) data.

Parameter	Value	Parameter	Value
Curb weight	1162 kg	C	0.41 N/(m/s)^2
r_{wheel}	0.28 m	Battery Pack Energy	2.1 kWh
A	104.49 N	$ICE_{maxpow,base}$	90 kW
B	2.43 N/(m/s)	$EM_{maxpow,base}$	30 kW

It is worth mentioning that, concerning the vehicle mass, a variation Δm has been considered as a function of ICE size, EM size, and the number of gears. Therefore, starting from the baseline value (i.e., a five-speed transmission, a 90 kW ICE, and a 30 kW EM), Δm has either been subtracted or added depending on the sizes of components for the candidate HEV powertrain design. The formulas used for this purpose are found below and have been extracted from [14]:

$$\Delta m_i = \Delta m_{transm,i} + \Delta m_{ICE,i} + \Delta m_{EM,i}, \tag{1}$$

$$\Delta m_{transm,i} = (5 - z_i) \cdot 0.12 \cdot ICE_{maxpow.base}, \tag{2}$$

$$\Delta m_{ICE,\,i} = 1.75 \cdot \left(ICE_{maxpow,base} - ICE_{maxpow,i} \right), \tag{3}$$

$$\Delta m_{EM,i} = 0.53 \cdot \left(EM_{maxpow,base} - EM_{maxpow,i} \right), \tag{4}$$

where z_i, $ICE_{maxpow,i}$, and $EM_{maxpow,i}$ are the number of gears, the ICE, and the EM peak powers of the i-th HEV candidate, respectively; $\Delta m_{transm,\,i}$, $\Delta m_{ICE,\,i}$, and $\Delta m_{EM,i}$ are instead the variation of mass due to the diverse number of gears and the different sizes of ICE and EM, respectively.

Concerning the modelling of the vehicle, a quasi-static approach was chosen that neglects transients to lower the computational cost. This method exploits the vehicle speed profile over time to compute the power request at the input shaft of the transmission. Equations (5) and (6) are used at each timestep for the aforementioned purpose:

$$T_{wheel} = \left(A + B\,v + C v^2 + m\,a + m\,g\,\sin(\alpha) \right) \cdot r_{dyn}, \tag{5}$$

$$T_{inp} = \frac{T_{wheel}}{\left(\tau_{diff} \cdot \tau_{gear}\right) \cdot \eta_{gear}{}^{sign\ (Twheel)}} \ , \tag{6}$$

where T_{wheel} and T_{inp} are the torques required at the wheel and at the input shaft of the transmission, respectively. v is the target velocity of the vehicle and *m* is the vehicle mass, while *a*, *g*, and *α* are the target acceleration, the gravity acceleration, and the road slope, respectively. *A*, *B*, and *C* are the coast down coefficients; τ_{diff} and τ_{gear} are the gear ratios of the differential and of the engaged gear; while η_{gear} is the transmission efficiency, which here is set to 90%. Once the torque required at the input shaft of the transmission is known, it is crucial to split this demand between the ICE and the EM as follows:

$$T_{del} = T_{ICE} \cdot \tau_{ICE} \cdot \gamma + T_{EM} \cdot (1 - \gamma) \tag{7}$$

where T_{del} is the torque delivered at the transmission input shaft by the two power sources, while τ_{ICE} is the gear ratios between ICE and the transmission. γ is the split term, for which values of 0 and 1 relate to pure electric mode and pure thermal mode, respectively. A value of γ lower than 1 denotes power assist torque split mode, while battery charging is performed when γ is greater than 1 and, in this case, the EM performs as an alternator. Using the knowledge of torque provided by the ICE and its rotational speed, the instantaneous fuel consumption can be found through the brake specific fuel consumption (BSFC) map. Regarding the electrical energy consumption, the battery power demand is computed first in Equation (8), then the instantaneous variation in state of charge (SOC) is calculated in Equation (9) as follows:

$$P_{batt} = (\omega_{EM} \cdot T_{EM}) + \mathcal{L}_{EM} + P_{aux} \tag{8}$$

$$\dot{SOC} = \frac{V_{oc} - \sqrt{V_{oc}^2 - 4R_{in}P_{batt}}}{2R_{in}Q_{batt}\Delta t} \tag{9}$$

where ω_{EM} is the rotational speed of the electric machine; $\mathcal{L}_{EM}$ represents the electrical power loss and it is derived empirically from the characteristic tables as a function of the torque and speed of the EM. P_{aux} represents the auxiliaries power request, set to 200 W for this study. Concerning the variation in SOC, it is computed in Equation (9) using the equivalent open circuit approach, where V_{oc}, R_{in}, and Q_{batt} are the open circuit voltage, the internal resistance, and the battery capacity (expressed in A/s), respectively; Δt is the simulation timestep.

2.2. HEV Control Level: DP

When it comes to the HEV control level, a DP-based algorithm was chosen as the strategy to compute the optimal torque split and gear engaged of each HEV candidate through the different drive cycles. This optimizer runs the drive mission backwards and, at every time step,

- It sweeps all the discretized control values;
- Then, it computes the state values for all the combinations of controls using the vehicle modeling equations given in the section above;
- Finally, it calculates a user-defined cost function that depends on the abovementioned values.

Then, the objective of this algorithm is to find the optimal time trajectories for gear number and torque split that minimize the cost function while complying with the imposed constraints [15,16]. In (10), the state space X, the control space U, and the cost function J_{DP} used for this study are found.

$$X = \left\{ \begin{array}{c} ICE_{state} \\ SOC \\ n_{gear} \end{array} \right\}, \quad U = \left\{ \begin{array}{c} n_{gear} \\ \gamma \end{array} \right\}, J_{DP} = \int_0^{t_{end}} \left(FC + \alpha_1 \cdot \mu_{gearshift} + \alpha_2 \cdot \mu_{ICE,on/off} \right) dt \tag{10}$$

X is composed of three variables, i.e., the binary ICE activation state (either on or off), the discretized battery SOC, and the gear engaged. U embeds again the gear engaged and the torque split term γ introduced in Equation (7). Lastly, J_{DP} is the cost function to be minimized throughout the overall driving mission up to its final time instant t_{end}. J_{DP} not only holds the instantaneous fuel consumption FC as obtained by interpolating in the ICE BSFC map, but it also considers two penalty terms aimed at improving drivability and comfort. These two terms are composed of the flags $\mu_{gearshift}$ and $\mu_{ICE,on/off}$ that are triggered when gear-shifting and ICE activation are encountered, respectively. α_1 and α_2 are constant weight factors for the respective penalty terms. Thus, the control strategy defined by the DP will not only be optimized for the fuel consumption, but it also will reduce both the number of gear shifts and ICE activations, in order to improve passengers' comfort. Finally, as already mentioned, the DP-based optimizer accounts for operational constraints and accepts only the control trajectories for which

- The ICE, the EM, and the battery operate within the corresponding operating limits;
- The actual vehicle velocity matches the trajectory imposed by the drive cycle;
- Final and initial battery SOC values are similar in simulating charge-sustaining HEV operation.

3. HEV Powertrain Bi-Nested Design Methodology

In this chapter, the focus is dedicated to the PSO and its cost function used for sizing the HEV. In the different subsections, there will be an explanation of the preliminary tests that each candidate has to pass before assessing its fuel economy and how the two main costs are computed.

3.1. HEV Design Level: PSO

Evolutionary algorithms (EAs) have been demonstrated to be capable of efficiently exploring the solution space of different optimization problems in several heterogeneous fields. For this reason, a PSO algorithm was chosen for the proposed research work as the HEV powertrain design optimizer. Skillfully sweeping the design parameters of the HEV and efficiently searching for an optimal layout is enabled in this way [17]. Among the different EAs, PSO was particularly selected owing to the reduced number of parameters to be tuned, which in turn fosters the possibility of finding the global optimal solution for the considered HEV design problem. Regarding the virtual environment, the PSO-based script was implemented in MATLAB® [18] together with the model of the HEV described by the data and formulas mentioned in the previous section. In this algorithm, each HEV design candidate is represented by an individual of the swarm population and has two main properties: a position and a velocity. Concerning the former, it embeds the sizing parameters, which can be found hereby in Table 2, whereas the velocity of the individual depends on the personal and global best positions, i.e., the positions in which the optimal cost function was found for both the single individual and the whole swarm. Regarding the parameters found in Table 2 below, the first two parameters EM_{size} and ICE_{size} are the sizes of the two power sources, EM and ICE, respectively; z represents the number of gears in the gearbox; $\tau_{g,1}$ and $\tau_{g,end}$ are the first and last gear ratios, respectively; and $\tau_{ICEtoTransm}$ and τ_{diff} are the ratios of the gear between the ICE and the transmission and the one at the differential. It is also worth mentioning that if a one-speed transmission is chosen by the PSO, $\tau_{g,end}$ is discarded, whereas if more than two gears are simulated, the "progressive gear step" method is applied to compute the intermediate ratios [19].

Table 2. Particle swarm optimization (PSO) design parameters and their ranges.

Parameter	Lower Bound	Upper Bound
EM size multiplier coefficient, EM_{size}	2	30
ICE size multiplier coefficient, ICE_{size}	45	180
Number of gears, z	1	6
First gear ratio, $\tau_{g,1}$	2.5	5.0
Last gear ratio, $\tau_{g,end}$	0.2	3.0
ICE to transmission ratio, $\tau_{ICEtoTransm}$	1.0	5.0
Differential ratio, τ_{diff}	1.0	4.0

For the sake of clarity, in Figure 2, the complete design workflow is found. More in detail, the swarm population is made of 100 individuals. Once the HEV design cost function has been assessed for each of them, an iteration of the algorithm ends and the positions of the individuals are updated according to their speeds. This mechanism allows the swarm to learn and to evolve intelligently owing to the formulation of the individual velocity. The excessive computational time deriving from the utilization of the DP led to the adoption of two stop criteria in the PSO algorithm. The optimization loop ends after 20 generations or if a steady-state solution has been found, i.e., when the best solution has not updated in the last five PSO iterations. In doing so, either an exhaustive part of the design space has been analyzed or an interesting design has been found.
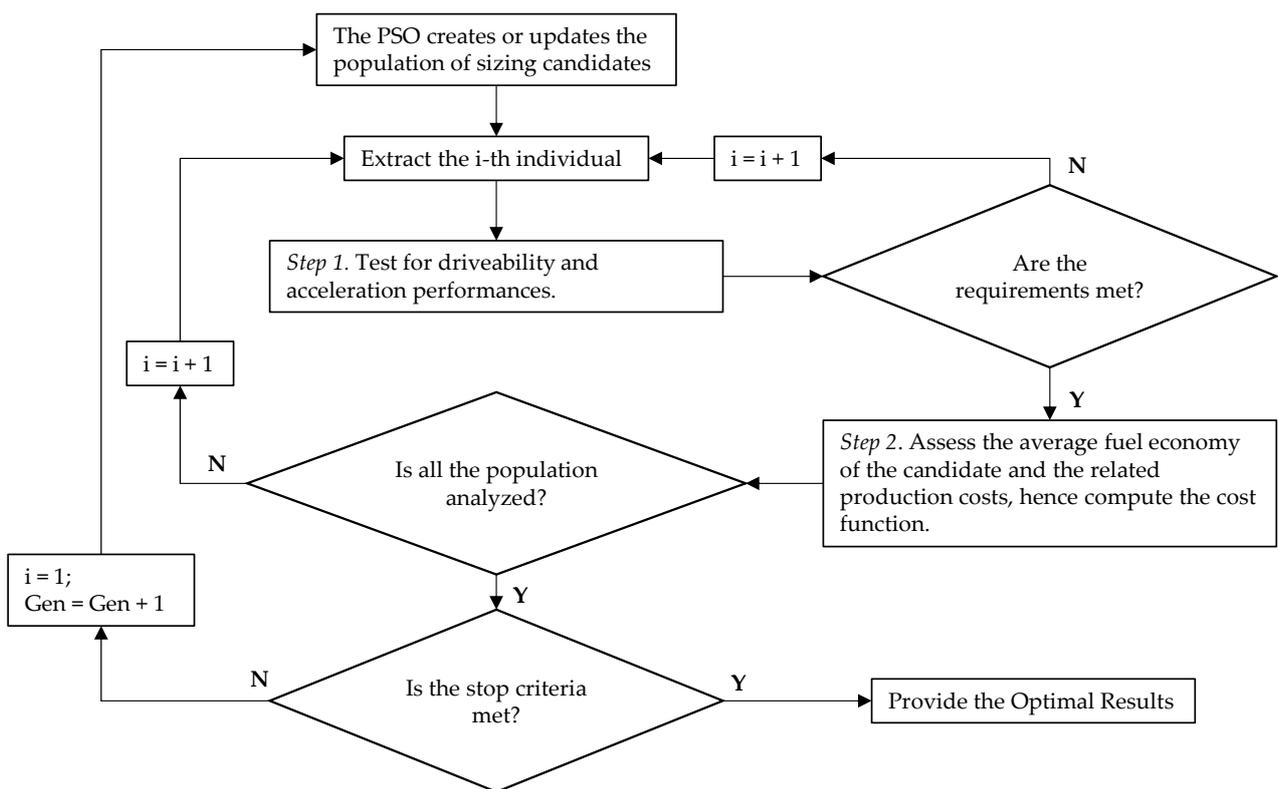

Figure 2. Complete design workflow.

Finally, the core of the study lies in the cost function implemented in the PSO, which is carefully designed to represent the different aspects to be optimized. It is basically made of two parts, i.e., the operative cost throughout the vehicle lifetime (set to 200,000 km here) and the HEV production cost. The objective is to obtain the least of the two combined costs, thus the considered optimization problem is a minimization one in which the best solution corresponds to the one with the lowest value among all of them. In this context, a

remarkably large value of the cost function, representative of infinite, has been assigned to the unfeasible individuals (i.e., HEV candidate). The formula of the cost function to be minimized using PSO is expressed in Equation (11) as follows:

$$J_{PSO} = w_{oper} \cdot cost_{oper} + w_{prod} \cdot cost_{prod} \tag{11}$$

where $cost_{oper}$ and $cost_{prod}$ are the HEV operative and production related costs, respectively. The procedures to calculate both of these HEV cost contributions will be discussed in detail in the following three sub-sections. w_{oper} and w_{prod} are weights applied to the respective HEV cost terms. In order to provide a broader view of the HEV design possibilities, the HEV design process using PSO illustrated in Figure 2 is repeated here four times by varying values of w_{oper} and w_{prod} in order to identify four different HEV powertrain layouts: (1) a totally fuel economy-oriented (TFO) HEV, (2) a mostly fuel economy-oriented (MFO) HEV, (3) a mostly production cost-oriented (MPO) HEV, and (4) a totally production cost-oriented (TPO) HEV. It is also worth mentioning that, even in design layouts predominantly oriented to fuel economy only or production cost only (i.e., TFO and TPO), the respective HEV cost term that is not optimized does provide a small percentage in the objective function, i.e., the corresponding weight is not null, yet close to zero. Furthermore, with the two contributions of the cost function being crucial for the understanding of the research, they will be thoroughly discussed in the following subsections, preceded by the explanation of the preliminary tests performed.

3.2. Preliminary Tests

Before simulating the driving missions to estimate the average fuel economy of an HEV individual, this has to overgo a few preliminary tests that assess the HEV drivability. To this end, the four tasks that need fulfillment by the HEV powertrain design candidate are presented in Table 3. These are taken from [20] while adapting the requirements to a class A passenger car. Tests are performed to prove the capability of the vehicle to overcome steep roads at different velocities and to ensure the capability of charge-sustaining the battery even at a high vehicle speed. Moreover, the time required to complete a 0–100 km/h maneuver is performed using a vehicle model implemented in SIMULINK® to assess the acceleration performance of each design candidate. More in detail, this latter test is performed at wide open throttle (i.e., providing maximum power from both ICE and EM) and the gear-shift is carefully implemented in order to deliver the highest overall propelling torque at each timestep. Only the HEV candidates successfully passing all four drivability tasks and achieving a 0–100 km/h time lower than 15 s are then evaluated in terms of fuel economy capability.

Table 3. Task required to be completed by the HEV in the drivability test.

Task #	Road Slope [%]	Task Explained
1	30	Perform a standing start
2	0	Maintain 150 km/h vehicle speed
3	7	Maintain 80 km/h vehicle speed
4	0	Charge-sustain the battery at 130 km/h

3.3. Production Cost

Concerning the production cost, it is strictly correlated to the sizes of the power sources and the transmission characteristics. The following equations were extracted from [14] to calculate the different factors contributing to the cost of production of an HEV:

$$cost_{prod} = ICE_{cost} + EM_{cost} + Transm_{cost} + Batt_{cost} + \ldots\ldots + cost_{base} + penalty_{CO2} \tag{12}$$

$$ICE_{cost} = 12.83 \cdot ICE_{maxpow} + 566 \tag{13}$$

$$EM_{cost} = 19.71 \cdot EM_{maxpow} + 417.5 \tag{14}$$

$$Transm_{cost} = [3.11 + 1.24 \cdot (z - 1)] \cdot ICE_{maxpow} \tag{15}$$

where the power values are expressed in kW, the results are in dollars (later converted into euro using a converter factor taken from the European Central Bank [21]), and all the coefficients shown are meant for a compact size vehicle. Concerning the terminology, ICE_{cost}, EM_{cost}, and $Transm_{cost}$ are the production costs related to the ICE, the EM, and the transmission; $Batt_{cost}$ and $cost_{base}$ are two constant terms (i.e., 615 $ and 10,325 $, which corresponds to almost 9000 €) and they account for the battery cost and a base price owing to chassis, wheels, other components, and accessories, which comes from [14]. Furthermore, $penalty_{CO2}$ is a penalty added to the production cost related to the CO_2 emission; this was computed only if the HEV candidate exceeds the threshold of 95 gCO_2/km imposed by the European Union for the 2020–21 target [22]. The amount of this penalty is set to 95 € for each gCO_2/km of target exceedance and, even though it is applied to a fleet in general, for the proposed study, it was considered for the single HEV candidate. Besides, in order to assess the emissions of each vehicle, a worldwide harmonised light vehicles test procedure (WLTP) was selected. Using the information related to the fuel consumption of the HEV in this mission as provided by DP, it is possible to estimate the CO_2 emissions of the design candidate. In the case in which this value is lower than 95 gCO_2/km, no penalty is considered and the production cost is simply Equation (12) without the last term. On the other hand, an additional vehicle cost contribution is included, being proportional to the estimated CO_2 emissions in the case wherein these are found to exceed European Union regulatory limits.

3.4. Operative Cost

Regarding the operative cost, it is correlated here with the average fuel consumption of the HEV candidate, which is assessed through different driving missions. For the purpose of this study, the considered missions are all real-world ones obtained using a global positioning System (GPS) in the city of Turin, Italy, and surrounding areas in the Piedmont region. More specifically, the three different missions are named 'urban cycle', 'uphill cycle', and 'highway cycle', and they are intended to represent diverse driving environments (i.e., urban, highway, and uphill), hence enriching the exhaustiveness of the fuel economy evaluation. 'Uphill cycle' contains not only information on vehicle velocity and acceleration over time, but also the net road altitude, which is accounted in the resistive force to be overcome by the vehicle. For the sake of clarity, in Figures 3–5, the vehicle speed profiles over time for the three missions are shown, whereas in Table 4, the main characteristics of each mission are reported. In particular, the trip duration and kilometrical lengths are given along with the minimum and maximum values of the acceleration, the highest velocity in the mission, and the variation in altitude shown only for the "uphill" cycle (Figure 4). This last term is to be intended as the difference between the altitude at the end of the mission and that at the starting point.
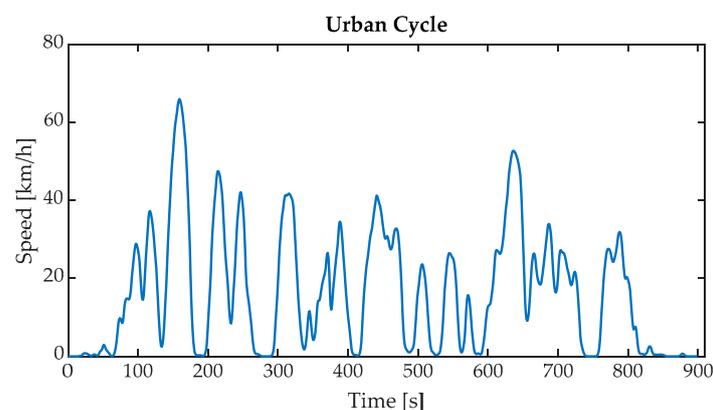

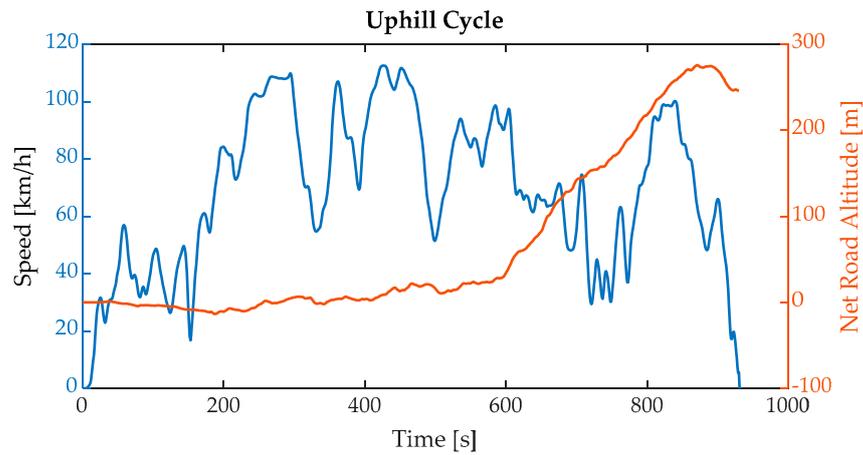**Figure 3.** Speed profile of the urban real-world drive mission.

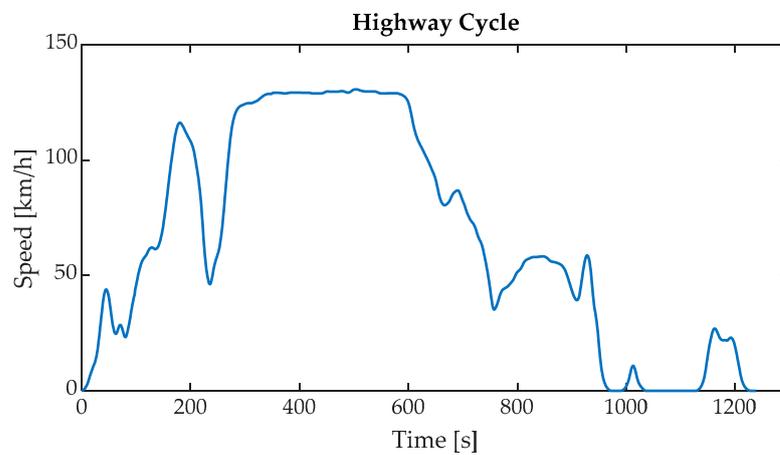**Figure 4.** Speed profile and net road altitude variation of the uphill real-world drive mission.

Figure 5. Speed profile of the highway real-world drive mission.

Table 4. Real-world drive mission main characteristics.

Cycle	Duration	Length	Accel. Range	Max Speed	Altitude Variation
Urban	900 s	4.1 km	$[-1.7, 1.4]$ m/s^2	66 km/h	/
Uphill	931 s	17.8 km	$[-1.7, 1.3]$ m/s^2	113 km/h	246 m
Highway	1240 s	22.9 km	$[-1.0, 0.8]$ m/s^2	131 km/h	/

In order to account for typical driving habits of a person when computing the average fuel economy, the following computation was developed. The aim here is to focus on the routine of a worker, hence working days are differentiated from weekends and holidays. In the former, the person drives only in the urban environment for commuting, thus the first cycle found in Table 4 accounts for 100% of fuel economy. On the other hand, regarding weekend and holidays, an average of the simulated fuel economies obtained for the three drive missions is used where higher weights are attributed to the "highway" and "uphill" cycles. Moreover, to address the variation in FE due to the number of persons inside the vehicle, it was added to the curb weight:

- The average mass of a person (i.e., 80 kg) when simulating the urban cycle (solo driving to work);
- The average mass of four persons when simulating the remaining cycles, thus simulating a family trip.

Lastly, considering 11 working months in a year and the remaining 1 as weekend or holiday, the following final average FE was computed:

$$FE_{avg} = 0.83 \cdot FE_{urb} + 0.09 \cdot FE_{HW} + 0.08 \cdot FE_{uphill} \tag{16}$$

where FE_{urb}, FE_{HW}, and FE_{uphill} are the fuel economy values obtained by the HEV candidate in 'urban cycle', 'highway cycle', and 'uphill cycle', respectively. As can be seen from Equation (16), the highest contribution is given by the urban cycle because of the fact that 11 months per year are spent mostly working (excluding the weekends), and thus driving in a city environment.

4. Results

In this section, the results obtained for the four different HEV design targets implemented in the PSO are found in a Pareto frontier. At first, a glimpse of how the HEV is controlled is provided by showing the main variables over a given drive mission. Then, a discussion about the results is provided to analyze the different optimal layouts of the HEV computed by the design algorithm.

4.1. HEV Control Level Decisions: Example

In Figures 6 and 7, an example of the HEV control trajectories identified by DP during the WLTP is shown considering two different vehicle layouts embedding a two-speed and a four-speed gearbox, respectively. These two differ not only in the transmission, but also in the powertrains: the sizes of the ICE and EM are 68 kW and 14 kW, respectively, in the two-speed HEV and 99 kW and 29 kW, respectively, in the four-speed vehicle.
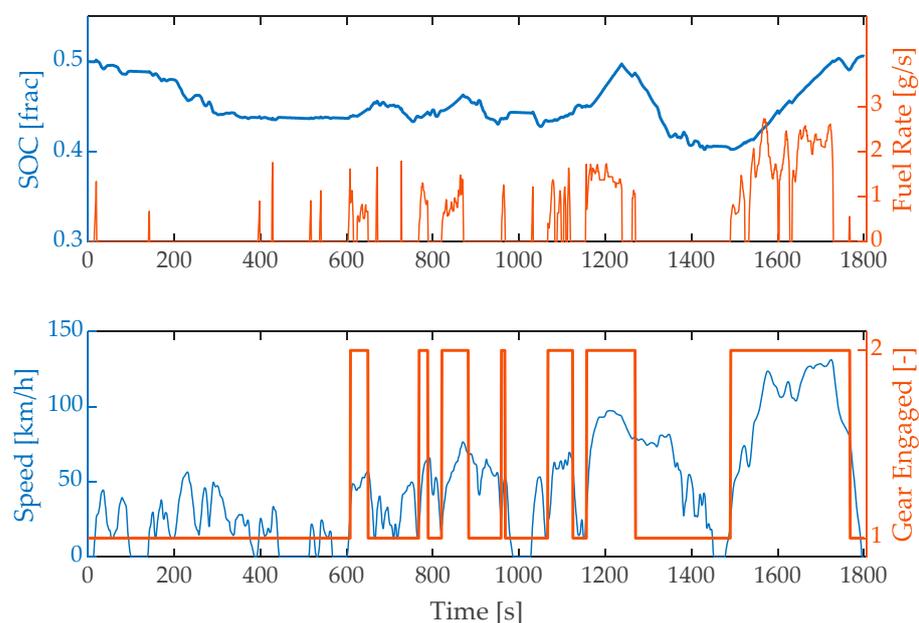

Figure 6. Example of the DP control results for a two-speed HEV driving the worldwide harmonised light vehicles test procedure (WLTP), equipped with a 68 kW ICE and a 14 kW EM.

More precisely, concerning the figures, on the top half of each, the SOC and the fuel rate are reported, providing information on the battery and ICE usage, whereas on the bottom, the speed profile of the drive cycle together with the engaged gear is shown. Focusing on the activation time of the ICE, it is roughly 29% of the overall drive mission when referring to the four-speed layout, against 27% with the two-speed HEV. Despite the longer running time of the former, it operates the ICE at higher efficiency points, obtaining an average fuel rate of 0.34 g/s in comparison with 0.38 g/s computed with the two-speed HEV (i.e., 10% higher in the average value throughout the WLTP). Thus,

it allows a lower amount of battery power to be recharged by the ICE to satisfy the SOC constraints. More details about the operative points in the brake specific fuel consumption map of the two ICEs mentioned above will be provided in Section 4.2. It might also be noted that the instantaneous fuel rate of the two-speed HEV reaches lower peaks, yet this is expected because the two ICEs are diverse in size. Moreover, a visible difference in SOC trend is found, especially focusing on the behavior of the two HEVs from 1200 s until the cycle ending. In this particular time window, the two-speed vehicle prefers to charge the battery at first, then discharge it to approximately 40%, and then it uses the ICE to bring the battery up to the initial SOC. Instead, with the four-speed vehicle, the battery is kept in a thinner SOC window and there is neither substantial usage nor recharge in electric energy.

A laptop computer equipped with Intel Core i7-9850H (2.6 GHz) and 16 GB of RAM was used to virtually simulate the vehicles. Regarding the two-speed HEV, it needed about 3 min for running the DP-based algorithm, whereas the four-speed took more than 16 min.
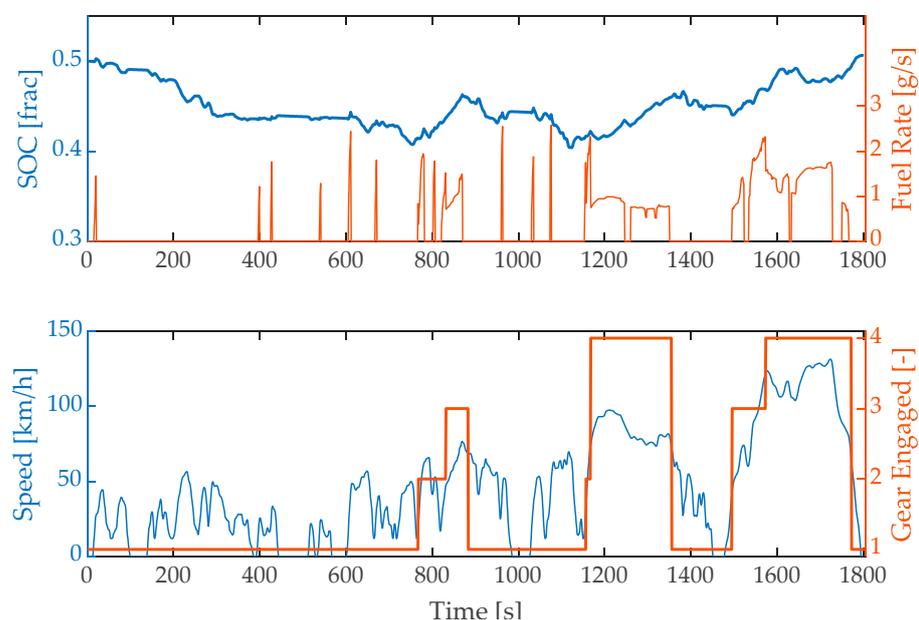

Figure 7. Example of the DP control results for a four-speed HEV driving the WLTP, equipped with a 99 kW ICE and a 29 kW EM.

4.2. PSO Results

The optimal HEV layouts resulting from the PSO algorithm for the four different design targets (i.e., TFO, MFO, MPO, TPO) are shown in Figure 8 as a Pareto frontier for average fuel economy and HEV production cost. As already stated in Section 3.1, the different HEV designs are oriented fully or mostly towards one of the two costs to be optimized, i.e., the production or the operative ones. This is performed by varying the value of w_{gasol} in the PSO objective function considering four discretized values ranging from 0.05 to 0.95 and repeating the entire HEV design workflow. Before presenting the final results obtained, it may be helpful to point out that about 24 days (i.e., approximately 570 h of computation) were dedicated to the design of the four different HEV layouts. To this end, the adoption of the PSO made possible an overall time reduction by guiding the sizing "evolution", still providing exhaustive outcomes.
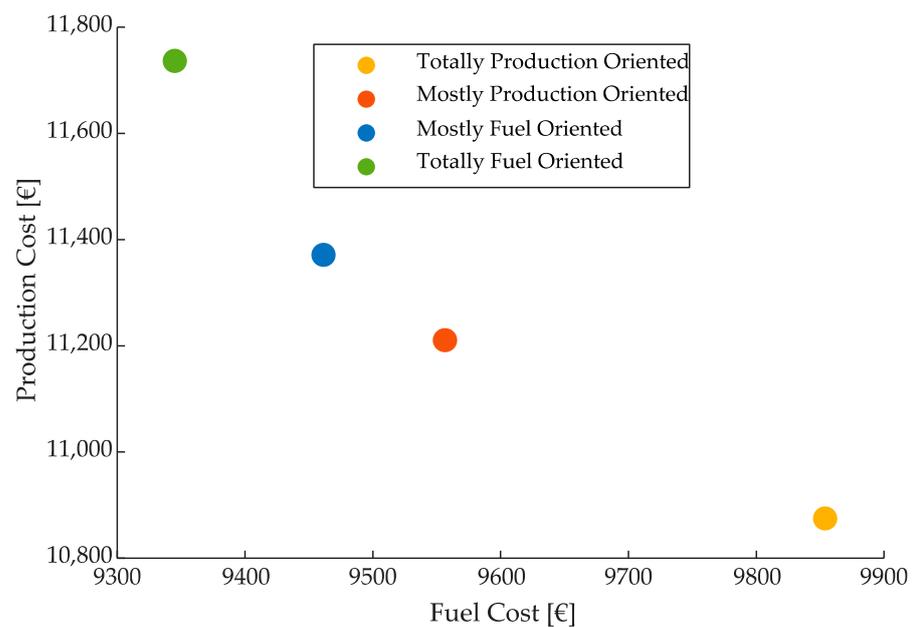
Figure 8. HEV optimal layouts for the different objective functions implemented in the PSO algorithm expressed in a Pareto frontier.

As seen in Figure 8, the two HEV layouts identified by PSO as TFO and TPO exhibit considerably different results in terms of production and fuel-related costs. This confirms the quality of PSO as design algorithm, which is able to intelligently optimize the different sizing parameters. The sizing parameters for the different optimal HEV powertrain layouts identified by the PSO are found in Table 5, along with additional information (i.e., HEV production cost, HEV fuel related cost, average fuel economy, and CO_2 penalty). In this table, the first layout corresponds to the totally production cost-oriented objective function (TPO), whereas the fourth is the totally fuel economy-oriented one (TFO). More in detail, the TPO HEV layout resulted in 10,875 € in production cost and 9854 € for the lifetime operative cost. On the opposite side, the TFO HEV layout obtained 11,736 € in cost due to the production (which corresponds to 860 € more than the previous design), yet the operative price dropped by about 500 €, resulting in 9345 €. Moreover, the two "middle" designs resulted in similar costs and their absolute differences are approximately 160 € regarding the production cost and about 90 € concerning the operative costs. No CO_2 penalties were added to any optimal layout as all resulted in an emission value below the threshold.

Table 5. Optimal HEV layouts' parameters.

Parameters	TPO	MPO	MFO	TFO
ICE size [kW]	68	71	80	99
EM size [kW]	14	27	30	29
Number of Gears	2	3	3	4
First Gear Ratio	3.52	3.92	2.58	2.95
Last Gear Ratio	0.73	0.37	0.46	0.54
Final Drive Ratio	2.61	2.22	2.61	2.29
ICE-Transm Ratio	2.17	1.56	1.42	1.11
Prod. Cost [€]	10,875	11,210	11,371	11,736
Fuel Cost. [€]	9854	9556	9461	9345
Avg. FE [L/100km]	3.39	3.29	3.26	3.22
CO_2 penalty	/	/	/	/

It might be worth reasoning on the choice of the PSO to the outcome of a four-speed HEV for the totally fuel economy-oriented layout. In this scenario, it is crucial to remember

that, even in the TFO HEV design case, a small percentage in the PSO objective function is assigned to the non-optimized cost (i.e., the production cost in this framework), the benefits in average fuel economy of having higher number of gears are shadowed by the substantial increase in production cost.

As a general trend observed in Table 5, the more importance given to the lifetime operative cost, the larger the size of both ICE and EM and the higher the number of gears in the transmission. This behavior might be partially explained by the capability of these HEV powertrain designs to shift the ICE operating points towards more efficient areas, owing to both the higher number of gears (i.e., the larger flexibility on ICE speed) and the higher torque deliverable by the EM, which in turn allows fine tuning the ICE torque to reduce fuel consumption.

The explanation just provided for fuel economy enhancement due to larger ICE, EM, and to higher number of gears is also supported by Figure 9, in which the WTLP operating points of the ICE for the four different identified HEV powertrain layouts are shown. In these graphs, the efficiency is given as brake specific fuel consumption (BSFC) and, as usual, the torque is reported as function of speed. It is to be noted that, although the maps look equal, the scale on the ordinate axis changes according to the ICE size.
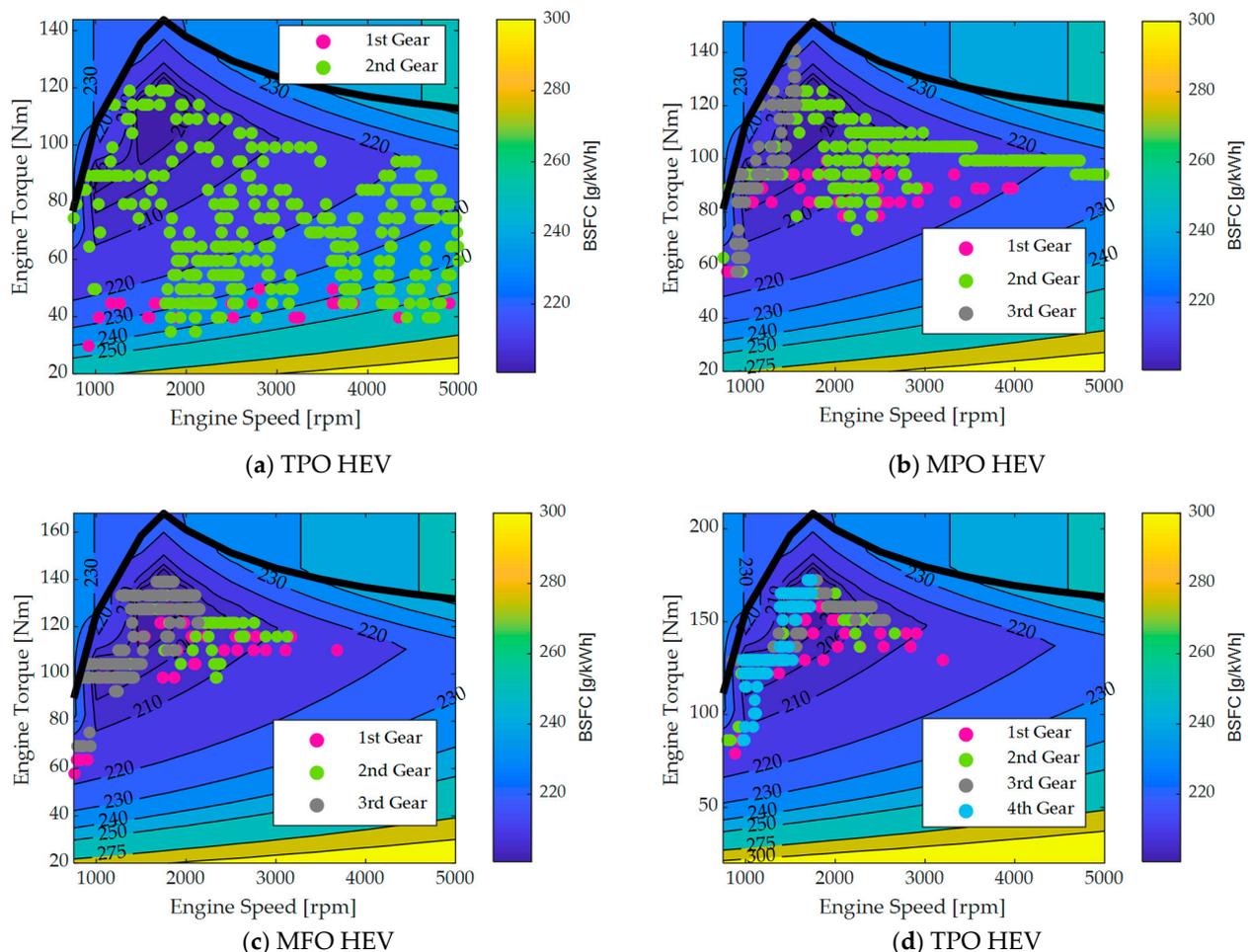

Figure 9. ICE operating point obtained in the WLTP drive mission for the (**a**) totally production-oriented, (**b**) mostly production-oriented, (**c**) mostly fuel-oriented, and (**d**) totally fuel-oriented optimal layouts. The colored map shows the brake specific fuel consumption (BSFC) areas, whereas the solid black line instead is the WOT curve.

A marked shift of the operating points can be progressively observed going from Figure 9a–d as the importance given to the operative cost is gradually increased. In Figure 9a, the ICE operating points for the TPO HEV design are found to be spread over

the BSFC map, even in low efficiency areas owing to small sizes in ICE and EM and to the reduced number of gears in the transmission. Instead, in Figure 9d, the obtained ICE operating points for the TFO HEV design are close to the most efficient BSFC zone, thus allowing a substantial improvement in fuel economy at the expense of the overall HEV production costs owing to larger ICE and EM sizes and a higher number of gears in the transmission.

5. Conclusions

This paper proposes an comprehensive and reliable design process for addressing the optimal P2 HEV layout of a class A vehicle for four different design targets. The sizing of the parameters is carried out through an evolutionary algorithm called PSO, whereas the energy management is provided according the DP process. Each HEV powertrain design candidate (or individual) has to be tested in drivability and acceleration to firstly ensure its driving feasibility. Then, its fuel economy capability is assessed using DP and considering real-world driving missions and the typical yearly driving habits of a user. The results show a large diversity in sizing parameters when different weights are assigned to conflicting HEV design targets such as overall vehicle production and fuel economy capability. When down-sizing ICE and EM and embedding a reduced number of gears in the AMT to limit HEV production cost, larger fuel consumption is generally observed owing to the ICE being constrained to operate in less efficient BSFC points. Nevertheless, a reduced number of gears in the AMT compared with a conventional engine-powered vehicle is suggested to be effective for an HEV thanks to the coordinated interaction between EM and ICE. Indeed, the outcomes for the HEV under design suggest that more than four gears would not be needed. This is mainly because of the fact that further enhancing the HEV fuel economy capability would not be possible without largely increasing the overall vehicle production cost. However, this statement should be related to the considered real-world driving scenarios (i.e., urban uphill and highway) and it might need further verification if different driving conditions were encountered by the HEV.

Related future work could consider using different HEV control strategies to lower the computational cost derived from the usage of DP, thus enhancing the computational efficiency for the HEV design parameters exploration. Equivalent consumption minimization strategy (ECMS) [23], slope-weighted energy-based rapid control analysis (SERCA) [24], or similar computationally-efficient HEV control strategies could find implementation in this framework. Car manufacturers might exploit this reliable design process to address the optimal HEV powertrain layout problem in this way. Besides, it might be interesting to study how the variation in HEV powertrain architecture (e.g., P1, P2, P3, and P4) impacts the HEV design outcomes, or to consider a different average fuel economy computation involving different customer habits.

Conflicts of Interest: The authors declare no conflict of interest.

References

1. Singh, K.V.; Bansal, H.O.; Singh, D. A comprehensive review on hybrid electric vehicles: Architectures and components. *J. Mod. Transport.* **2019**, *27*, 77–107. [CrossRef]
2. Anselma, P.G.; Belingardi, G. *Next Generation HEV Powertrain Design Tools: Roadmap and Challenges*; SAE Technical Paper 2019-01-2602; SAE: Warrendale, PA, USA, 2019. [CrossRef]
3. Roy, H.K.; McGordon, A.; Jennings, P.A. A Generalized Powertrain Design Optimization Methodology to Reduce Fuel Economy Variability in Hybrid Electric Vehicles. *IEEE Trans. Veh. Technol.* **2014**, *63*, 1055–1070. [CrossRef]

4. Yoon, Y.; Kim, K.; Kim, S. *Clutchless Geared Smart Transmission*; SAE Technical Paper 2011-01-2031; SAE: Warrendale, PA, USA, 2011. [CrossRef]

5. Kim, S.J.; Kim, K.; Kum, D. Feasibility Assessment and Design Optimization of a Clutchless Multimode Parallel Hybrid Electric Powertrain. *IEEE/ASME Trans. Mechatron.* **2016**, *21*, 774–786. [CrossRef]

6. Wood, E.; Alexander, M.; Bradley, T.H. Investigation of battery end-of-life conditions for plug-in hybrid electric vehicles. *J. Power Sources* **2011**, *196*, 5147–5154. [CrossRef]

7. Zhou, Q.; Zhang, W.; Cash, S.; Olatunbosun, O.; Xu, H.; Lu, G. Intelligent sizing of a series hybrid electric power-train system based on Chaos-enhanced accelerated particle swarm optimization. *Appl. Energy* **2017**, *189*, 588–601. [CrossRef]

8. Gao, W.; Porandla, S.K. Design optimization of a parallel hybrid electric powertrain. In Proceedings of the 2005 IEEE Vehicle Power and Propulsion Conference, Chicago, IL, USA, 7 September 2005. [CrossRef]

9. Spano, M.; Anselma, P.G.; Belingardi, G.; Misul, D.A.; Spessa, E. Assessing Lightweight Layouts for a Parallel Hybrid Electric Vehicle Driveline. In Proceedings of the 2020 AEIT International Conference of Electrical and Electronic Technologies for Automotive (AEIT AUTOMOTIVE), Turin, Italy, 18–20 November 2020; pp. 1–6. [CrossRef]

10. Fathy, H.K.; Reyer, J.A.; Papalambros, P.Y.; Ulsoy, A.G. On the coupling between the plant and controller optimization problems. In Proceedings of the American Control Conference, Arlington, VA, USA, 25–27 June 2001; Volume 3, pp. 1864–1869.

11. Liu, J.; Peng, H. Control optimization for a power-split hybrid vehicle. In Proceedings of the American Control Conference, Minneapolis, MN, USA, 14–16 June 2006.

12. Lin, C.-C.; Peng, H.; Grizzle, J.W.; Kang, J.-M. Power management strategy for a parallel hybrid electric truck. *IEEE Trans. Control Syst. Technol.* **2003**, *11*, 839–849. [CrossRef]

13. Anselma, P.G.; Belingardi, G.; Falai, A.; Maino, C.; Miretti, F.; Misul, D.; Spessa, E. Comparing Parallel Hybrid Electric Vehicle Powertrains for Real-world Driving. In Proceedings of the 2019 AEIT International Conference of Electrical and Electronic Technologies for Automotive (AEIT AUTOMOTIVE), Torino, Italy, 2–4 July 2019; pp. 1–6.

14. Finesso, R.; Misul, D.; Spessa, E.; Venditti, M. Optimal Design of Power-Split HEVs Based on Total Cost of Ownership and CO_2 Emission Minimization. *Energies* **2018**, *11*, 1705. [CrossRef]

15. Bellman, R.E.; Lee, E. History and development of dynamic programming. *Control Syst. Mag.* **1984**, *4*, 24–28. [CrossRef]

16. Sundstrom, O.; Guzzella, L. A generic dynamic programming Matlab function. In Proceedings of the 2009 IEEE Control Applications, (CCA) & Intelligent Control (ISIC), St. Petersburg, Russia, 8–10 July 2009; pp. 1625–1630. [CrossRef]

17. Kennedy, J.; Eberhart, R. Particle swarm optimization. In Proceedings of the ICNN'95—International Conference on Neural Networks, Perth, WA, Australia, 27 November–1 December 1995; Volume 4, pp. 1942–1948. [CrossRef]

18. Kalami Heris, M. Particle Swarm Optimization in MATLAB. Available online: https://yarpiz.com/50/ypea102-particle-swarm-optimization (accessed on 22 March 2021).

19. Lechner, G.; Naunheimer, H. *Automotive Transmissions, Fundamentals, Selection, Design and Applications*; Springer: Berlin/Heidelberg, Germany, 2010; pp. 89–90.

20. Anselma, P.G.; Biswas, A.; Bruck, L.; Bonab, S.A.; Lempert, A.; Roeleveld, J.; Madireddy, K.; Rane, O.; Wasacz, B.; Belingardi, G.; et al. Accelerated Sizing of a Power Split Electrified Powertrain. *SAE Int. J. Adv. Curr. Prac. Mobil.* **2020**, *2*, 2701–2711.

21. European Central Bank. Euro Foreign Exchange Reference Rates, US Dollar. Available online: https://www.ecb.europa.eu/stats/policy_and_exchange_rates/euro_reference_exchange_rates/ (accessed on 27 May 2021).

22. European Commission. Reducing CO_2 Emissions from Passenger Cars—Before 2020. Available online: https://ec.europa.eu/clima/policies/transport/vehicles/ (accessed on 26 March 2021).

23. Onori, S.; Serrao, L.; Rizzoni, G. Adaptive equivalent consumption minimization strategy for hybrid electric vehicles. In Proceedings of the Dynamic Systems and Control Conference, Cambridge, MA, USA, 12–15 September 2010; Volume 44175, pp. 499–505.

24. Anselma, P.G.; Biswas, A.; Belingardi, G.; Emadi, A. Rapid assessment of the fuel economy capability of parallel and series-parallel hybrid electric vehicles. *Appl. Energy* **2020**, *275*, 115319. [CrossRef]